

Document downloaded from the institutional repository of the University of Alcalá: <https://ebuah.uah.es/dspace/>

This is a postprint version of the following published document:

Wang, Qiqin et al., 2014. Enantioseparation of N-derivatized amino acids by micro-liquid chromatography using carbamoylated quinidine functionalized monolithic stationary phase. *Journal of Chromatography A*, 1363, pp.207–215.

Available at <https://doi.org/10.1016/j.chroma.2014.06.039>

© 2014 Elsevier

(Article begins on next page)



This work is licensed under a
Creative Commons Attribution-NonCommercial-NoDerivatives
4.0 International License.

Accepted Manuscript

Title: Enantioseparation of *N*-derivatized amino acids by micro-liquid chromatography using carbamoylated quinidine functionalized monolithic stationary phase

Author: Qiqin Wang Jun Feng Hai Han Peijie Zhu Huihui Wu
María Luisa Marina Jacques Crommen Zhengjing Jiang



PII: S0021-9673(14)00963-7
DOI: <http://dx.doi.org/doi:10.1016/j.chroma.2014.06.039>
Reference: CHROMA 355518

To appear in: *Journal of Chromatography A*

Received date: 14-4-2014
Revised date: 12-6-2014
Accepted date: 12-6-2014

Please cite this article as: Q. Wang, J. Feng, H. Han, P. Zhu, H. Wu, M.L. Marina, J. Crommen, Z. Jiang, Enantioseparation of *N*-derivatized amino acids by micro-liquid chromatography using carbamoylated quinidine functionalized monolithic stationary phase, *Journal of Chromatography A* (2014), <http://dx.doi.org/10.1016/j.chroma.2014.06.039>

This is a PDF file of an unedited manuscript that has been accepted for publication. As a service to our customers we are providing this early version of the manuscript. The manuscript will undergo copyediting, typesetting, and review of the resulting proof before it is published in its final form. Please note that during the production process errors may be discovered which could affect the content, and all legal disclaimers that apply to the journal pertain.

1 **Enantioseparation of *N*-derivatized amino acids by**
2 **micro-liquid chromatography using carbamoylated**
3 **quinidine functionalized monolithic stationary phase**

4
5 Qiqin Wang^{1,2#}, Jun Feng^{1#}, Hai Han¹, Peijie Zhu¹, Huihui Wu¹, María Luisa Marina², Jacques
6 Crommen^{1,3}, Zhengjing Jiang^{1,*}

7
8 ¹*Department of Pharmacy and Guangdong Province Key Laboratory of Pharmacodynamic*
9 *Constituents of Traditional Chinese Medicine & New Drug Research, Jinan University,*
10 *Guangzhou 510632, China*

11 ²*Department of Analytical Chemistry, Physical Chemistry and Chemical Engineering, Faculty of*
12 *Biology, Environmental Sciences and Chemistry, University of Alcalá, Ctra. Madrid-Barcelona,*
13 *Km. 33.600, 28871 Alcalá de Henares (Madrid), Spain*

14 ³*Laboratory of Analytical Pharmaceutical Chemistry, Department of Pharmaceutical Sciences,*
15 *University of Liege, CHU B36, B-4000 Liege, Belgium*

16
17 * *Corresponding author*

18 *Tel.: +86 2085223604*

19 *E-mail address: jzjjackson@hotmail.com*

20
21 # *These authors contributed equally to this work.*

40 **Abstract:**

41 In order to obtain satisfactory column permeability, efficiency and selectivity for
42 micro-HPLC, a capillary monolithic column containing
43 *O*-9-[2-(methacryloyloxy)-ethylcarbamoyl]-10,11-dihydroquinidine (MQD) as chiral
44 selector was re-optimized. The monolithic column was used to successfully
45 enantioresolve a wide range of *N*-derivatized amino acids including alanine, leucine,
46 methionine, threonine, phenylalanine, valine, serine, isoleucine, tryptophan, and
47 cysteine. The influence of mobile phase parameters, such as the organic solvent type
48 and concentration, the apparent pH, and buffer concentration, on retention and
49 enantioseparation of *N*-derivatized amino acids has been investigated.
50 3,5-dinitrobenzoyl-amino acids and 3,5-dichlorobenzoyl-amino acids were resolved
51 into enantiomers with exceptionally high selectivity and resolution. The
52 chemoselectivity of the monolithic column for a multicomponent mixture of
53 *N*-derivatized amino acids was also investigated. A mixture of three pairs of
54 3,5-dichlorobenzoyl-amino acids could be fully resolved in 22.5 minutes.

55

56

57 **Keywords:** carbamoylated quinidine / enantioseparations / *N*-derivatized amino
58 acids / monolithic columns / micro-HPLC

59

59 1. Introduction

60 The stereochemistry of amino acids plays an important role in their biological and
61 pharmacological properties. An increasing number of observations suggests that
62 *D*-amino acids have a significant influence in living organisms, including humans [1].
63 Some *D*-amino acids have been found to be related to different diseases, including
64 schizophrenia [2], Alzheimer's disease [3] and renal disorders [4]. For example,
65 *D*-serine may be useful as a biomarker and even a therapeutic agent for neurological
66 disorders [5], while *L*-serine plays a key role in the central nervous system and cellular
67 proliferation [6]. Moreover, amino acids as chiral building blocks have a significant
68 importance for synthetic therapeutic peptides [7]. However, it is difficult to resolve
69 free amino acids into their enantiomers because of an obvious lack of appropriate
70 functionalities to interact with the chiral selectors [8]. In order to enhance the
71 intermolecular interaction between amino acids and chiral selectors, additional
72 interaction sites could be introduced through the derivatization of amino groups [9],
73 using reagents such as carbazole-9-carbonyl (CC) chloride [9], 2,4-dinitrophenyl
74 (DNP) fluoride [10], 4-fluoro-7-nitro-2,1,3-benzoxadiazole (NBD-F) [11], or dansyl
75 (DNS) chloride [12]. These UV-absorbing or fluorescent derivatization agents could
76 also bring a strong chromophore or fluorophore into amino acids and peptides for
77 improving detection sensitivity [9,13]. Therefore, the enantioseparation of
78 *N*-derivatized amino acids remains a hot research topic even if well advanced. A series
79 of chiral stationary phases (CSPs), containing polysaccharides [14], macrocyclic
80 antibiotics [15], native or cationic cyclodextrins (CD) [16], and
81 (*S*)-*N*-3,5-dinitrobenzoyl-1-naphthylglycine [17] as chiral selectors, have been applied
82 to the enantioseparation of different kinds of *N*-derivatized amino acids. In particular,
83 carbamoylated quinine and quinidine immobilized on silica microparticles have
84 received great attention due to their excellent enantioselectivity towards various kinds
85 of acidic analytes, such as *N*-derivatized amino acids [18-19], profens [20], α -aryloxy
86 alkanolic acids [18], 1,4-dihydropyridine monocarboxylic acid [21], pyrethroid acids
87 [22], *N*-derivatized peptides [23], dafachronic acids [24], and aminophosphonic acids
88 [25]. The enantioselectivity could be attributed to a global effect, including ion-pair
89 formation between chiral analytes and selector, dipole-dipole, hydrophobic, hydrogen
90 bonding, π - π and steric interactions [26].
91 In the last decade, monolithic columns have proved to be an effective alternative to

92 packed columns and have attracted considerable interest owing to their facile
93 preparation methodology and good column characteristics, such as permeability and
94 efficiency [27]. Lämmerhofer et al. developed quinine and quinidine-based chiral
95 monolithic columns, namely poly
96 (O-9-(*tert*-butylcarbamoyl)-11-[2-(methacryloyloxy)ethylthio]
97 -10,11-dihydroquinine-*co*-2-hydroxyethyl methacrylate-*co*-ethylene dimethacrylate)
98 and poly
99 (O-9-[2-(methacryloyloxy)-ethylcarbamoyl]-10,11-dihydroquinidine-*co*-2-hydroxyethyl
100 methacrylate-*co*-ethylene dimethacrylate) (poly(MQD-*co*-HEMA-*co*-EDMA)) for
101 capillary electrochromatography (CEC) applications by *in situ* copolymerization of
102 O-9-(*tert*-butylcarbamoyl)-11-[2-(methacryloyloxy)ethylthio]-10,11-dihydroquinine
103 or O-9-[2-(methacryloyloxy)-ethylcarbamoyl]-10,11-dihydroquinidine [12,28]. These
104 macroporous chiral monolithic columns exhibited very good enantioselectivity and
105 column efficiency in the CEC mode for several *N*-derivatized amino acids, such as
106 CC-Alanine, CC-Serine, and 3,5-dinitrobenzoyl (DNB)-Leucine [12,28-30]. However,
107 their applicability to micro-HPLC separations does not seem to have been
108 investigated so far. It is well known that the column properties required for
109 micro-HPLC are different from those for CEC. Therefore, a systematic optimization
110 of the polymerization conditions is required in order to obtain satisfactory
111 micro-HPLC performance with respect to column permeability, mechanical stability,
112 efficiency and selectivity. Besides, it is of high interest to systematically evaluate the
113 enantioselectivity of poly(MQD-*co*-HEMA-*co*-EDMA) monolithic columns towards a
114 wider range of analytes since only a few derivatives of leucine and valine have been
115 examined so far [12,28-30].

116 In this study, a capillary liquid chromatography column containing carbamoylated
117 quinidine was prepared according to Lämmerhofer et al [28]. In order to obtain
118 satisfactory column permeability, efficiency and selectivity in micro-HPLC, the
119 composition of the polymerization mixture was re-optimized. The optimized
120 monolithic column was subsequently applied to the enantioseparation of various kinds
121 of *N*-derivatized amino acids, containing benzoyl (B), *p*-nitrobenzoyl (*p*-NB),
122 3,5-dinitrobenzoyl (3,5-DNB), 3,5-dimethoxybenzoyl (3,5-DMB),
123 9-fluorenylmethoxycarbonyl (Fmoc), 3,5-dichlorobenzoyl (3,5-DCIB),
124 *m*-chlorobenzoyl (*m*-ClB), *p*-chlorobenzoyl (*p*-ClB), or *o*-chlorobenzoyl (*o*-ClB)
125 protecting groups. The influence of the organic solvent type and content, the buffer

126 concentration and the apparent pH of the mobile phase on the enantioseparation of
127 these amino acid derivatives has also been investigated. The separation mechanism is
128 also discussed on the basis of a comparison of the influence of the type of
129 *N*-protecting group and amino acid on enantioseparation.

130

131 **2. Experimental**

132 **2.1. Chemicals and materials**

133 3-(Trimethoxysilyl)-propyl methacrylate (γ -MAPS), 2,2'-azobisisobutyronitrile
134 (AIBN), 2-hydroxyethyl methacrylate (HEMA), ethylene dimethacrylate (EDMA),
135 methanol (MeOH), dodecanol, chloroform, cyclohexanol, acetonitrile (ACN), acetic
136 acid, ammonium formate, ammonium acetate and dibutyltin dilaurate were all
137 purchased from Aladdin Chemicals (Shanghai, China). 4-Methoxyphenol and
138 2-isocyanatoethyl methacrylate were obtained from Maya Reagent (Jiaxing, Zhejiang,
139 China). All racemic amino acids (alanine, leucine, methionine, threonine,
140 phenylalanine, valine, serine, isoleucine, tryptophan, and cysteine),
141 10,11-dihydroquinidine (DHQD) and nine aryl chlorides (*p*-nitrobenzoyl chloride,
142 3,5-dinitrobenzoyl chloride, 3,5-dimethoxybenzoyl chloride,
143 9-fluorenylmethoxycarbonyl chloride, 3,5-dichlorobenzoyl chloride, *m*-chlorobenzoyl
144 chloride, *p*-chlorobenzoyl chloride, benzoyl chloride, and *o*-chlorobenzoyl chloride)
145 were purchased from Energy Chemical (Shanghai, China). All *N*-derivatized amino
146 acids were synthesized according to a standard procedure [31] except Fmoc and
147 3,5-DCIB derivatives. As described previously [32], amino acids were amidated by
148 9-fluorenylmethoxycarbonyl chloride in aqueous solution to afford Fmoc-derivatized
149 amino acids. 3,5-DCIB derivatives were synthesized through reaction of amino acids
150 with 3,5-dichlorobenzoyl chloride in THF [33]. Distilled water was filtered through a
151 2- μ m membrane before use. The fused-silica capillaries (375 μ m O.D. \times 100 μ m I.D.)
152 were obtained from Ruifeng Chromatography Ltd. (Yongnian, Hebei, China).

153

154 **2.2. Instrumentation**

155 All scanning electron microscopy (SEM) experiments were carried out using an
156 ultra-high resolution Hitachi S-4800 SEM (Tokyo, Japan) at an acceleration
157 voltage of 1 kV. A Jinghong DK-S22 water bath (Shanghai, China) was used for
158 thermally initiated copolymerization. All micro-HPLC experiments were carried out

159 on a self-assembled HPLC system that consisted of a DiNa nano gradient pump
160 (Tokyo, Japan), a Valco four-port injection valve with 20 nL internal loop (Houston,
161 TX, USA), and a Shimadzu SPD-15C UV detector (Kyoto, Japan). Data acquisition
162 and data handling were performed using a Unimicro TrisepTM Workstation 2003
163 (Shanghai, China). All chromatograms were converted to a text file and redrawn using
164 Microcal Origin 8.0. The pH values were monitored by a Sartorius PB-10 pH meter
165 (Gottingen, Germany).

166

167 **2.3. Chromatographic conditions**

168 Unless otherwise stated, the mobile phase was a mixture of ACN/0.1 M ammonium
169 acetate (80/20; v/v). The mobile phase apparent pH was adjusted to the desired value
170 by adding acetic acid. All chiral samples were dissolved in MeOH to reach a final
171 concentration around 1 mg/mL. The mobile phase was filtered through a 0.22- μ m
172 membrane and degassed before use. The flow rate of the mobile phase was set at 1
173 μ L/min and the injection volume was 20 nL. The analytes were all detected at a
174 wavelength of 254 nm.

175

176 **2.4. Preparation of poly(MQD-*co*-HEMA-*co*-EDMA) monolithic columns**

177 **2.4.1. Synthesis of**

178 ***O*-[2-(Methacryloyloxy)ethylcarbamoyl]-10,11-dihydroquinidine**

179 The functional monomer MQD was synthesized according to Lämmerhofer et al.
180 [28] using a properly modified procedure. In brief, 2-isocyanatoethyl methacrylate
181 (1.4 mL, 10 mmol) was added to a mixture of DHQD (1.3 g, 4 mmol), dibutyltin
182 dilaurate (10 drops) and 4-methoxyphenol (10 mg) in THF (30 mL), followed by
183 stirring for 96 h at room temperature. The mixture was filtered, concentrated under
184 reduced pressure. The residue was purified on a packed silica column using a eluent
185 consisting of chloroform /MeOH (40:1; v/v) to afford MQD (white powder, yield
186 58.7%).

187

188 **2.4.2. Preparation of poly(MQD-*co*-HEMA-*co*-EDMA) monolithic columns**

189 The monomers (MQD, HEMA, and EDMA), the binary porogenic mixture
190 (1-dodecanol and cyclohexanol) and the initiator AIBN (1 wt% with respect to the
191 monomers) were mixed ultrasonically into a homogenous solution in a 2-mL vial. The
192 composition of the polymerization mixture was optimized in order to obtain

193 satisfactory permeability and selectivity (**Table 1**). After sonication and bubbling with
194 nitrogen for 5 min, this polymerization mixture was transferred into a 20-cm long
195 capillary, which had been pretreated with γ -MAPS in order to afford anchoring sites
196 for the polymeric bulk [34-35]. The filled capillaries were sealed with GC septa and
197 submerged into a water bath at 60 °C for 20 h. The obtained monolithic columns were
198 then flushed out using MeOH in order to remove unreacted chemicals and porogens.
199 A 2-3 mm detection window was created at a distance of 3 cm from the end of the
200 column using a thermal wire stripper. The capillary column was cut into a total length
201 of 18 cm with an effective length of 15 cm. The finally obtained bulk polymer was
202 taken for elemental analysis. A 3-5 mm length of monolith was then cut, placed on an
203 aluminum stub and then sputter-coated with gold for SEM analysis.

204

205 **2.5. Calculations**

206 The enantioselectivity (α) was calculated according to the following expression: $\alpha =$
207 k_2/k_1 where $k = (t_R - t_0)/t_0$ (t_0 is the elution time of the solvent peak, which was used as
208 the dead time, t_{R1} , t_{R2} , k_1 and k_2 are the retention times and the retention factors of the
209 first and second eluting enantiomers, respectively) [34]. The theoretical plate number
210 (N) and the resolution factor (R_s) were determined according to the standard equations
211 based on their corresponding widths at half-height [36].

212

213 **3. Results and discussion**

214 **3.1. Preparation and optimization of poly(MQD-co-HEMA-co-EDMA)** 215 **monolithic columns**

216 Lämmerhofer et al. previously prepared successfully a quinidine-based chiral
217 monolithic column for enantioseparations in the CEC mode [28]. However, a column
218 with satisfactory performance in CEC might not be suitable for a successful HPLC
219 separation. The permeability is a very important property of an HPLC column
220 because of its direct and indirect influence on a number of factors, such as stability,
221 analysis time, column efficiency, resolution etc. In order to obtain a poly
222 (MQD-co-HEMA-co-EDMA) monolithic column with satisfactory permeability and
223 efficiency in micro-HPLC, the composition of the polymerizable mixture was
224 re-optimized as shown in **Table 1** by evaluating the properties and structure of the
225 monoliths using micro-HPLC and SEM.

226 In order to investigate the effect of the porogens in the reaction mixture, the weight
227 content of the binary porogenic mixture was varied from 70% (C1) to 60% w/w (C3)
228 while the composition of monomers and porogens was kept constant. It was observed
229 that the decrease of the total weight content of porogens resulted in a clear increase of
230 the backpressure from 2.9 MPa to 10.1 MPa. Column C2 exhibited a suitable
231 backpressure and the highest column efficiency (24400 theoretical plates/m at a linear
232 flow rate of 1.1 mm/s using naphthalene as test compound) when compared to
233 columns C1 and C3.

234 It was also observed that the co-monomer HEMA affected the column performance.
235 As the weight fraction of HEMA in the monomers increased from 52.5% (C2) to
236 57.5% (C5) w/w, the theoretical plate number increased from 24400 to 32000
237 plates/m while the backpressure remained almost constant. A further increase of the
238 HEMA weight content to 60% (C6) caused a significant increase of backpressure and
239 a slight decrease in column efficiency. Therefore, considering the column
240 permeability and efficiency, a HEMA weight content of 57.5% in the monomers was
241 selected for all further experiments.

242 The composition of the porogenic mixture (dodecanol/cyclohexane ratio) was also
243 taken into consideration. The micro-HPLC experiments showed that the column
244 backpressure increased from 5.8 MPa to 13.1 MPa when the content of dodecanol
245 decreased from 88.33% (C7) to 78.33% (C8) wt%. On the other hand, the best column
246 efficiency was obtained on column C5 with 83.33 % dodecanol in the porogenic
247 mixture.

248 Finally, a polymerization mixture consisting of 35 wt% monomers
249 (MQD/HEMA/EDMA, 20/57.5/22.5, w/w/w) and 65 wt% porogens
250 (dodecanol/cyclohexanol, 83.33/16.67, w/w) was chosen for all further studies since it
251 yielded the monolith C5 exhibiting uniform structure and good permeability and
252 efficiency. **Fig. 1a** and **Fig. 1b** shows the SEM result for column C5, where spherical
253 units agglomerate into large clusters interdispersed by large-pore channels.

254

255 **3.2. Permeability and reproducibility of poly(MQD-co-HEMA-co-EDMA)** 256 **monolithic columns**

257 The permeability of the poly(MQD-co-HEMA-co-EDMA) monolithic column was
258 determined by pumping ACN, MeOH, and water through it at different linear flow
259 rates. According to Bristow and Knox [37], the permeability K can be expressed as

260 follows:

$$261 \quad K = (uL/\Delta P)\eta$$

262 where η is the dynamic viscosity of the eluent, u is the linear velocity of the mobile
263 phase, L is the length of the column, and ΔP is the pressure drop across the column.

264 Since toluene was unretained in organic mobile phases, it was selected as dead-time
265 marker when ACN and MeOH were used as eluents. When using water as mobile
266 phase, thiourea was selected as t_0 marker. The good mechanical stability of column
267 C5 could be evidenced by the excellent linearity between backpressure and linear
268 velocity over the pressure range of 0-13 MPa (Figure not shown). The calculated K
269 values for column C5 are given in **Table 2**. The results indicate a high permeability
270 for the optimized poly(MQD-*co*-HEMA-*co*-EDMA) monolithic column, which is
271 ideal for HPLC applications.

272 In addition, the reproducibility of the poly(MQD-*co*-HEMA-*co*-EDMA) monolithic
273 columns was assessed by determining the relative standard deviations (RSDs) for the
274 retention factors of two test analytes, i.e. anisole and naphthalene. A mixture of
275 ACN/H₂O (40/60, v/v) was used as mobile phase. The RSD values for run to run ($n =$
276 10) repeatability of anisole and naphthalene retention factors were 0.88% and 1.08%,
277 respectively. The RSD values for day to day ($n=5$) repeatability were 2.18% and
278 2.78%, respectively. These data demonstrate the stability of the
279 poly(MQD-*co*-HEMA-*co*-EDMA) monolithic columns, since their properties do not
280 seem to change significantly either with time or with the number of injections.
281 Furthermore, the batch to batch ($n=3$) reproducibility values for anisole and
282 naphthalene retention factors were 4.38% and 4.47%, respectively. These results
283 further confirm the good reproducibility of the optimized
284 poly(MQD-*co*-HEMA-*co*-EDMA) monolithic columns.

285

286 **3.3. Effects of mobile phase composition on enantioseparation**

287 In order to systematically evaluate the enantioselectivity of the optimized
288 poly(MQD-*co*-HEMA-*co*-EDMA) monolithic columns in the micro-HPLC mode, two
289 *N*-derivatized amino acids, i.e. 3,5-DNB-Leucine and 3,5-DCIB-Leucine, were chosen
290 as test analytes. The influence of the organic solvent type and concentration, the
291 apparent pH and the buffer concentration was investigated.

292 The influence of the organic solvent type (MeOH and ACN) in the mobile phase on
293 retention times and enantioselectivity was first studied. Both 3,5-DNB-Leucine and

294 3,5-DCIB-Leucine could be enantioseparated with mixtures of either MeOH/0.1 M
295 ammonium acetate (80/20, v/v, apparent pH = 5.3) or ACN/0.1 M ammonium acetate
296 (80/20, v/v, apparent pH = 5.3) as mobile phase. However, the retention of the second
297 enantiomer of 3,5-DNB-Leucine was too high to be eluted from the column within
298 120 min when MeOH/0.1 M ammonium acetate (80/20, v/v, apparent pH = 5.3) was
299 used as mobile phase. Therefore ACN/H₂O system was chosen for studying the
300 influence of the organic solvent concentration on the enantioseparation of the two
301 *N*-derivatized amino acids. As can be seen in **Table 3**, the retention factors of both
302 analytes increased dramatically with decreasing ACN content from 80 to 60%.
303 However the enantioselectivity (α) remained fairly constant over the studied ACN
304 concentration range while the enantioresolution (R_s) increased with decreasing ACN
305 concentration, owing to increasing retention and column efficiency. This might
306 suggest that part of the retention on the poly(MQD-*co*-HEMA-*co*-EDMA) monolithic
307 stationary phase under the tested conditions is due to hydrophobic interaction and that
308 the latter is not responsible for enantioselectivity. In order to find the best compromise
309 between retention times and enantioresolution, a mobile phase containing 80% ACN
310 was considered as the most suitable for further experiments.

311 It has been reported that the electrostatic interactions between the negatively charged
312 carboxylate function of *N*-derivatized amino acids and the positively charged tertiary
313 nitrogen of quinidine play an important role in the enantioselectivity of
314 quinidine-based stationary phases [8]. The mobile phase pH could affect the
315 ionization state of both quinidine (pK_a = 8.72) [38] stationary phase and analytes, i.e.
316 3,5-DNB-Leucine (pK_a = 3.77) [39] and 3,5-DCIB-Leucine (pK_a = 3.79) [39].
317 Therefore its effect on the enantioseparation of the two *N*-derivatized amino acids was
318 also investigated by adjusting the apparent pH value of the mobile phase (ACN/0.1 M
319 ammonium acetate (80/20; v/v)) to 6.3, 5.3 and 4.3 after mixing with ACN. As shown
320 in **Table 4**, both retention factors (k_1 and k_2) and R_s of 3,5-DNB-Leucine and
321 3,5-DCIB-Leucine decreased with decreasing mobile phase apparent pH from 6.3 to
322 4.3. The α values remained almost constant between pH 6.3 and 5.3, and then
323 decreased significantly at pH 4.3. This behavior is certainly related to the fact that in
324 the selected apparent pH range, the quinidine stationary phase remains fully positively
325 charged while the negative charge of the two *N*-derivatized amino acids will start
326 decreasing with decreasing apparent pH, resulting in a reduction of electrostatic

327 interactions and hence of enantioselectivity. Finally, an apparent pH of 5.3 was
328 selected because it represented the best compromise between enantioresolution and
329 analysis time.

330 The influence of the buffer concentration was also investigated by varying the
331 concentration of ammonium acetate from 0.05 to 0.15 M, while the other
332 chromatographic conditions were kept constant (**Table 5**). No significant influence on
333 enantioselectivity for both *N*-derivatized amino acids was observed in this
334 concentration range. However, their retention and enantioresolution clearly increased
335 with decreasing ammonium acetate concentration. These results might indicate that
336 the contribution of electrostatic interactions to the retention of these acidic analytes
337 increases with decreasing concentration of the competing anion acetate. A 0.1 M
338 concentration of ammonium acetate was found to be the most suitable with respect to
339 enantioresolution and analysis time.

340

341 **3.4. Enantioseparation of *N*-derivatized amino acids**

342 In order to systematically evaluate the enantioselectivity of poly
343 (MQD-*co*-HEMA-*co*-EDMA) monolithic columns in the micro-HPLC mode, various
344 kinds of *N*-derivatized amino acids were synthesized and enantioseparated (**Table 6**).
345 The tagging reagents used to derivatize the amino acids included the following
346 *N*-protecting groups: B, *p*-NB, 3,5-DNB, 3,5-DMB, Fmoc, 3,5-DCIB, *m*-CIB, *p*-CIB
347 and *o*-CIB (**Fig. 2**).

348 The results (k_1 , k_2 , α , R_s , N_1 and N_2) obtained for 47 *N*-derivatized amino acids
349 (alanine, isoleucine, leucine, methionine, valine, threonine, phenylalanine, cysteine,
350 serine, and tryptophan derivatives) on poly (MQD-*co*-HEMA-*co*-EDMA) monolithic
351 columns are given in **Table 6**. Under the selected chromatographic conditions, 44 out
352 of 47 analytes could be baseline enantioresolved ($R_s > 1.5$), and the other three
353 analytes could be partially enantioseparated ($0.74 \leq R_s < 1.5$). The highest
354 enantioresolution values were observed for 3,5-DNB derivatives, followed by
355 3,5-DCIB derivatives. It was also noticed that the poly (MQD-*co*-HEMA-*co*-EDMA)
356 monolithic column optimized for micro-HPLC could offer a better enantioselectivity
357 within a shorter analysis time comparing with the previously reported poly
358 (MQD-*co*-HEMA-*co*-EDMA) monolithic column used in CEC [28]. For instance, α
359 value of ~ 2.91 and R_s value of ~ 8.44 for 3,5-DNB-Leucine enantiomers were
360 obtained over 40 minutes in the CEC mode [28], while α value of ~ 4.71 and R_s value

361 of ~ 8.51 for 3,5-DNB-Leucine enantiomers were reached less than 12 minutes in the
362 micro-HPLC mode. These results further demonstrate the great potential of the
363 poly(MQD-*co*-HEMA-*co*-EDMA) monolithic column to enantioresolve a wide range
364 of *N*-derivatized amino acids.

365 When the results in **Table 6** are more closely examined, a similar trend in
366 enantioselectivity for amino acid derivatives in each series was noticed. For instance,
367 α values for 3,5-DCIB amino acid enantiomers were in the following rank order:
368 isoleucine > valine > phenylalanine > leucine > tryptophan > methionine > threonine
369 > cysteine > alanine > serine. Lindner et. al. showed that the lipophilicity and
370 bulkiness of the side chain of the analytes may affect the enantiodiscrimination
371 potential of quinidine-based columns [8]. Furthermore, they found that an increase of
372 the size and bulkiness of the side chain leads to an enhancement in the retention of the
373 second eluting enantiomer [8]. Interestingly, a similar phenomenon was observed in
374 this study. For instance, the α -values for some aliphatic amino acid enantiomers as
375 3,5-DCIB derivatives increase in the order: serine (hydroxymethyl, $\alpha = 2.18$) <
376 cysteine (thiomethyl, $\alpha = 2.28$) < threonine (1-hydroxyethyl, $\alpha = 2.57$), and alanine
377 (methyl, $\alpha = 2.21$) < leucine (isobutyl, $\alpha = 3.12$) < isoleucine (*sec.*-butyl, $\alpha = 4.24$).

378 In order to study the influence of *N*-protecting groups on the enantioseparation, eight
379 different *N*-derivatized leucine derivatives were selected. As shown in **Table 7** and
380 **Fig. 3**, baseline enantioseparation could be achieved on the poly
381 (MQD-*co*-HEMA-*co*-EDMA) column for all eight analytes. Furthermore, the
382 enantioselectivity for the amino acid derivatives decreased with decreasing
383 electrophilic character of the *N*-protecting groups. This trend could be deduced from
384 the reduction of enantioselectivity obtained by exchanging the strong π -acidic
385 3,5-DNB groups for the weaker π -acidic *p*-NB and B groups: e.g. α
386 (3,5-DNB-Leucine) = 4.71 > α (*p*-NB-Leucine) = 1.74 > α (B-Leucine) = 1.34.
387 Lindner et. al. showed that the *N*-protecting groups could provide a strongly
388 electron-deficient aromatic system for π - π interaction with the quinoline ring of
389 quinidine [8]. The effective π - π interaction increment of the *N*-protecting groups
390 could improve the enantioselectivity for *N*-derivatized amino acids [8].

391 In order to confirm the enantiomer elution order, L-form enantio-enriched
392 3,5-DNB-Methionine and 3,5-DNB-Alanine were used as analytes. As can be seen in
393 **Fig. 4**, the L-enantiomers were always eluted first. The same enantiomer elution order
394 has been previously observed for 3,5-DNB-Leucine [28] and Fmoc-Leucine [29],

395 which suggests that the L-enantiomers are more or less excluded from the “binding
396 groove” of the quinidine moiety whereas the D-enantiomers better match the binding
397 sites [8].

398

399 **3.4.1. Chemoselectivity of the poly (MQD-*co*-HEMA-*co*-EDMA) monolithic** 400 **column**

401 A major limitation of CSPs is often their intrinsically limited chemoselectivity. In
402 order to evaluate the chemoselectivity of poly(MQD-*co*-HEMA-*co*-EDMA)
403 monolithic stationary phases, a mixture of 3,5-DCIB-Leucine, 3,5-DCIB-Valine, and
404 3,5-DCIB-Tryptophan enantiomers was tested under isocratic conditions in
405 micro-HPLC. **Fig. 5** shows that all three pairs of 3,5-DCIB amino acid enantiomers
406 could be completely separated in less than 22.5 minutes. Hence, the poly
407 (MQD-*co*-HEMA-*co*-EDMA) monolithic column can be used for the
408 enantioseparation of a multicomponent mixture of *N*-derivatized amino acids in the
409 micro-HPLC mode.

410

411 **4. Conclusion**

412 In this research, a capillary monolithic column containing carbamoylated quinidine as
413 chiral selector was re-optimized in order to obtain satisfactory column permeability,
414 efficiency and selectivity in micro-HPLC. The optimized poly
415 (MQD-*co*-HEMA-*co*-EDMA) monolithic column showed excellent morphology,
416 good permeability, reproducibility, mechanical and chemical stability and satisfactory
417 chromatographic performance in micro-HPLC. The influence of the organic solvent
418 content, the buffer concentration and the apparent pH of the mobile phase on the
419 retention and enantioseparation of *N*-derivatized amino acids seems to confirm that
420 both hydrophobic and electrostatic interactions are responsible for the retention of
421 these acidic analytes, while only the latter contribute to enantioselectivity. Based on a
422 comparison of the influence of the type of *N*-protecting groups and amino acids on
423 enantioseparation, it was deduced that the size and bulkiness of the side chain of
424 amino acids as well as the electrophilic character of the *N*-protecting groups are likely
425 to affect the enantiodiscrimination potential of the poly(MQD-*co*-HEMA-*co*-EDMA)

426 monolithic column. The optimized monolithic column was finally applied to the
427 enantioseparation of a wide range of *N*-derivatized amino acids with exceptionally
428 high selectivity values and good resolution, especially for 3,5-DNB-amino acids and
429 3,5-DCIB-amino acids. Good chemoselectivity of the monolithic column for a
430 multicomponent mixture of *N*-derivatized amino acids was also observed.

431

432 **5. Acknowledgements**

433 We gratefully appreciate the financial support from the National Natural Science
434 Foundation of China (Grants: 81273477 and 8120249) and the Science and
435 Technology Innovation Project of Guangdong Provincial Education Department
436 (Grant: 34312014).

437

438 **6. References**

- 439 [1] K. Hamase, A. Morikawa, K. Zaitso, J. Chromatogr. B 781 (2002) 73.
440 [2] S. Kato, Y. Kito, H. Hemmi, T. Yoshimura, J. Chromatogr. B 879 (2011) 3190.
441 [3] G. Fisher, N. Lorenzo, H. Abe, E. Fujita, W.H. Frey, C. Emory, M.M. Di Fiore, A.
442 D'Aniello, Amino acids 15 (1998) 263.
443 [4] H. Brückner, M. Hausch, J. Chromatogr. 614 (1993) 7.
444 [5] M. Friedman, C.E. Levin, Amino acids 42 (2012) 1553.
445 [6] T.J. de Koning, K. Snell, M. Duran, R. Berger, B.T. Poll-The, R. Surtees, Biochem.
446 J. 371 (2003) 653.
447 [7] R. Pell, S. Sić, W. Lindner, J. Chromatogr. A 1269 (2012) 287.
448 [8] M. Lämmerhofer, W. Lindner, J. Chromatogr. A 741 (1996) 33.
449 [9] C. Czerwenka, M. Lämmerhofer, W. Lindner, J. Sep. Sci. 26 (2003) 1499.
450 [10] C. Czerwenka, M. Lämmerhofer, W. Lindner, J. Pharmaceut. Biomed, 30 (2003)
451 1789.
452 [11] Y. Song, T. Funatsu, M. Tsunoda, J. Chromatogr. B 879 (2011) 335.
453 [12] M. Lämmerhofer, E. Tobler, E. Zarbl, W. Lindner, F. Svec, J.M.J. Fréchet,
454 Electrophoresis 24 (2003) 2986.
455 [13] A. Péter, E. Vékes, A. Árki, D. Tourwé, W. Lindner, J. Sep. Sci. 26 (2003) 1125.

- 456 [14] Y. Li, C. Baek, B.W. Jo, W. Lee, Bull. Korean Chem. Soc. 26 (2005) 998.
- 457 [15] I. Ilisz, R. Berkecz, A. Péter, J. Sep. Sci. 29 (2006) 1305.
- 458 [16] X. Yao, T.T. Tan, Y. Wang, J. Chromatogr. A 1326 (2014) 80.
- 459 [17] M. Kato, T. Fukushima, N. Shimba, I. Shimada, Y. Kawakami, K. Lmai, Biomed.
460 Chromatogr. 15 (2001) 227.
- 461 [18] K.M. Kacprzak, W. Lindner, J. Sep. Sci. 34 (2011) 2391.
- 462 [19] H. Hettegger, M. Kohout, V. Mimini, W. Lindner, J. Chromatogr. A 1337 (2014)
463 85.
- 464 [20] K.H. Krawinkler, E. Gavioli, N.M. Maier, W. Lindner, Chromatographia 58(2003)
465 555.
- 466 [21] M. Lämmerhofer, O. Gyllenhaal, W. Lindner, J. Pharmaceut. Biomed. 35 (2004)
467 259.
- 468 [22] W. Bicker, M. Lämmerhofer, W. Lindner, J. Chromatogr. A 1035 (2004) 37.
- 469 [23] K. Gyimesi-Forrás, K. Akasaka, M. Lämmerhofer, N.M. Maier, T. Fujita, M.
470 Watanabe, N. Harada, W. Lindner, Chirality 17 (2005) S134.
- 471 [24] R. Sardella, A. Carotti, A. Gioiello, A. Lisanti, F. Ianni, W. Lindner, B. Natalini, J.
472 Chromatogr. A 1339 (2014) 96.
- 473 [25] A. F. Gargano, M. Kohout, P. Maciková, M. Lämmerhofer, W. Lindner, Anal.
474 Bioanal. Chem. 405 (2013) 8027. [26] V. Piette, M. Lämmerhofer, K. Bischoff,
475 W. Lindner, Chirality 9 (1997) 157.
- 476 [27] Z. Jiang, N.W. Smith, Z. Liu, J. Chromatogr. A 1218 (2011) 2350.
- 477 [28] M. Lämmerhofer, E.C. Peters, C. Yu, F. Svec, J.M. Fréchet, Anal. chem. 72 (2000)
478 4614.
- 479 [29] M. Lämmerhofer, F. Svec, J.M.J. Fréchet, W. Lindner, J. Microcolumn Sep. 12
480 (2000) 597.
- 481 [30] M. Lämmerhofer, F. Svec, J.M. Fréchet, Anal. Chem. 72 (2000) 4623.
- 482 [31] B.S. Jursic, D. Neumann, Synthetic Commun. 31 (2001) 555.
- 483 [32] M.B. Gawande, P.S. Branco, Green Chem. 13 (2011) 3355.
- 484 [33] W.H. Pirkle, T.C. Pochapsky, J. Am. Chem. Soc. 109 (1987) 5975.
- 485 [34] Q. Zhang, J. Guo, F. Wang, J. Crommen, Z. Jiang, J. Chromatogr. A 1325 (2014)

486 147.

487 [35] Z. Jiang, N.W. Smith, P.D. Ferguson, M.R. Taylor, *Anal. Chem.* 79 (2007) 1243.

488 [36] V. Piette, M. Lämmerhofer, W. Lindner, J. Crommen, *J. Chromatogr. A* 987 (2003)

489 421.

490 [37] P.A. Bristow, J.H. Knox, *Chromatographia*, 10 (1977) 279.

491 [38] M. Lämmerhofer, P. Imming, W. Lindner, *Chromatographia*, 60 (2004) S13.

492 [39] <https://scifinder.cas.org/scifinder/view/scifinder/scifinderExplore.jsf>

493

Accepted Manuscript

493 **Figure captions**

494

495 **Fig. 1. Scanning electron microphotographs of column C5.**

496

497 **Fig. 2. Structures of amino acids and *N*-protecting groups.**

498

499 **Fig. 3. Enantioseparation of *N*-derivatized leucine derivatives on the**
500 **poly(MQD-*co*-HEMA-*co*-EDMA) monolithic column.** Conditions: column

501 dimensions: 150 mm × 100 μm I.D.; mobile phase: a). ACN/0.1 M ammonium acetate

502 (80/20, v/v) (apparent pH = 5.3) for all analytes except Fmoc-Leucine, b). ACN/0.1 M

503 ammonium acetate (50/50, v/v) (apparent pH = 5.3) for Fmoc-Leucine; UV detection

504 wavelength: 254 nm; flow rate: 1 μL/min; injection volume: 20 nL.

505

506 **Fig. 4. Elution order of 3,5-DNB-Methionine and 3,5-DNB-Alanine**
507 **enantiomers on the poly(MQD-*co*-HEMA-*co*-EDMA) monolithic column.**

508 Conditions: mobile phase, ACN/0.1 M ammonium acetate (80/20, v/v) (apparent pH =

509 5.3); other conditions as in **Fig. 3.**

510

511 **Fig. 5. Enantioseparation of 3,5-DCIB-Leucine, 3,5-DCIB-Valine and**
512 **3,5-DCIB-Tryptophan.** Conditions: flow rate: 0.5 μL/min; samples:

513 3,5-DCIB-Leucine (1, 4), 3,5-DCIB-Valine (2, 5) and 3,5-DCIB-Tryptophan (3, 6);

514 other conditions as in **Fig. 4.**

515

516 **Table 1. Composition of the polymerization mixtures used for the preparation of**
517 **poly(MQD-*co*-HEMA-*co*-EDMA) monolithic columns and their properties.**

518 Conditions: column dimensions: 150 mm × 100 μm I.D.; mobile phase, ACN/H₂O

519 (40/60, v/v); UV detection wavelength: 214 nm; flow rate: 1 μL/min; injection

520 volume: 20 nL; sample: naphthalene.

521

522

523 **Table 2. Permeability of the poly(MQD-*co*-HEMA-*co*-EDMA) monolithic column**

524 ^a Relative polarity data were obtained from
525 <http://virtual.yosemite.cc.ca.us/smurov/orgsoltab.htm>; viscosity data of pure solvents
526 were obtained from reference [32].

527

528 **Table 3. Effect of ACN content in the mobile phase on the retention and**
529 **enantioseparation of *N*-derivatized amino acids.** Conditions: column: 150 mm ×
530 100 μm I.D. poly(MQD-*co*-HEMA-*co*-EDMA); mobile phase: mixture of ACN and
531 0.1 M ammonium acetate at various ratios (apparent pH = 5.3); UV detection
532 wavelength: 254 nm; flow rate: 1 μL/min; injection volume: 20 nL.

533

534

535 **Table 4. Effect of the mobile phase apparent pH on the retention and**
536 **enantioseparation of *N*-derivatized amino acids.** Conditions: mobile phase,
537 ACN/0.1 M ammonium acetate (80/20, v/v) adjusted to different apparent pH values;
538 other conditions as in **Table 3**.

539

540

541

542 **Table 5. Effect of the buffer concentration on the retention and**
543 **enantioseparation of *N*-derivatized amino acids.** Conditions: ACN/different
544 concentrations of ammonium acetate (80/20, v/v) (apparent pH = 5.3); other
545 conditions as in **Table 3**.

546

547

548

549 **Table 6. Enantioseparation of *N*-derivatized amino acids.** Conditions: mobile
550 phase, ^aACN/0.1 M ammonium acetate solution (80/20, v/v) (apparent pH = 5.3); ^b
551 ACN/0.1 M ammonium acetate (50/50, v/v) (apparent pH = 5.3); ^c ACN/ 0.1 M
552 ammonium acetate (40/60, v/v) (apparent pH = 5.3); other conditions as in **Fig. 3**; “/”:
553 the number of theoretical plates cannot be calculated.

554

555 **Table 7. Comparison of retention factors, selectivity and enantioresolution for**
556 **different *N*-derivatized leucine derivatives.** Conditions as in **Fig. 3**.

594 Highlights

595 ♦ A carbamoylated quinidine based monolith was prepared for using in
596 micro-HPLC.

597 ♦ This monolithic column exhibited great properties for chromatographic
598 performance in micro-HPLC .

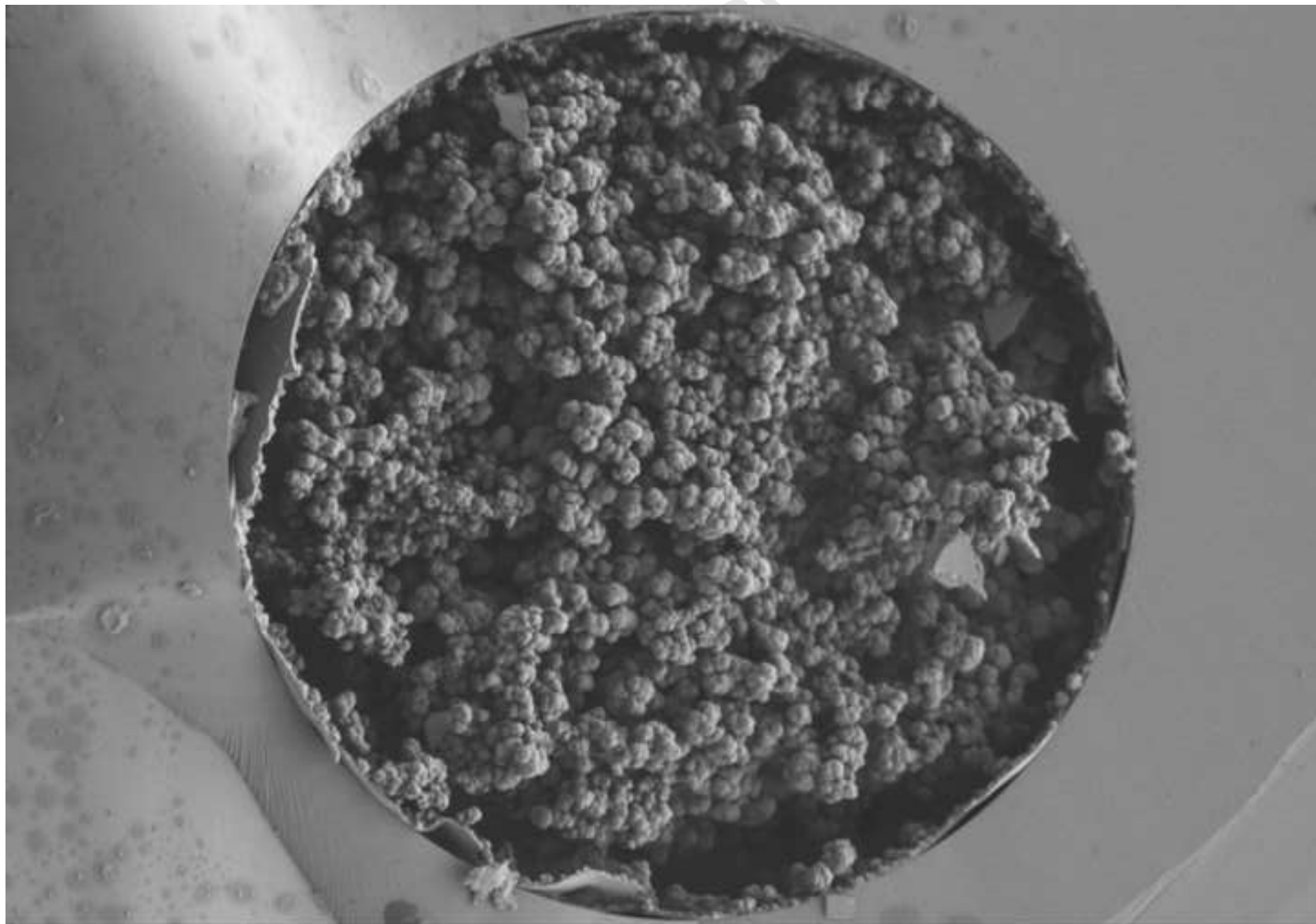
599 ♦ A wide range of *N*-derivatized amino acids were systematically evaluated and
600 successfully enantioresolved.

601

602

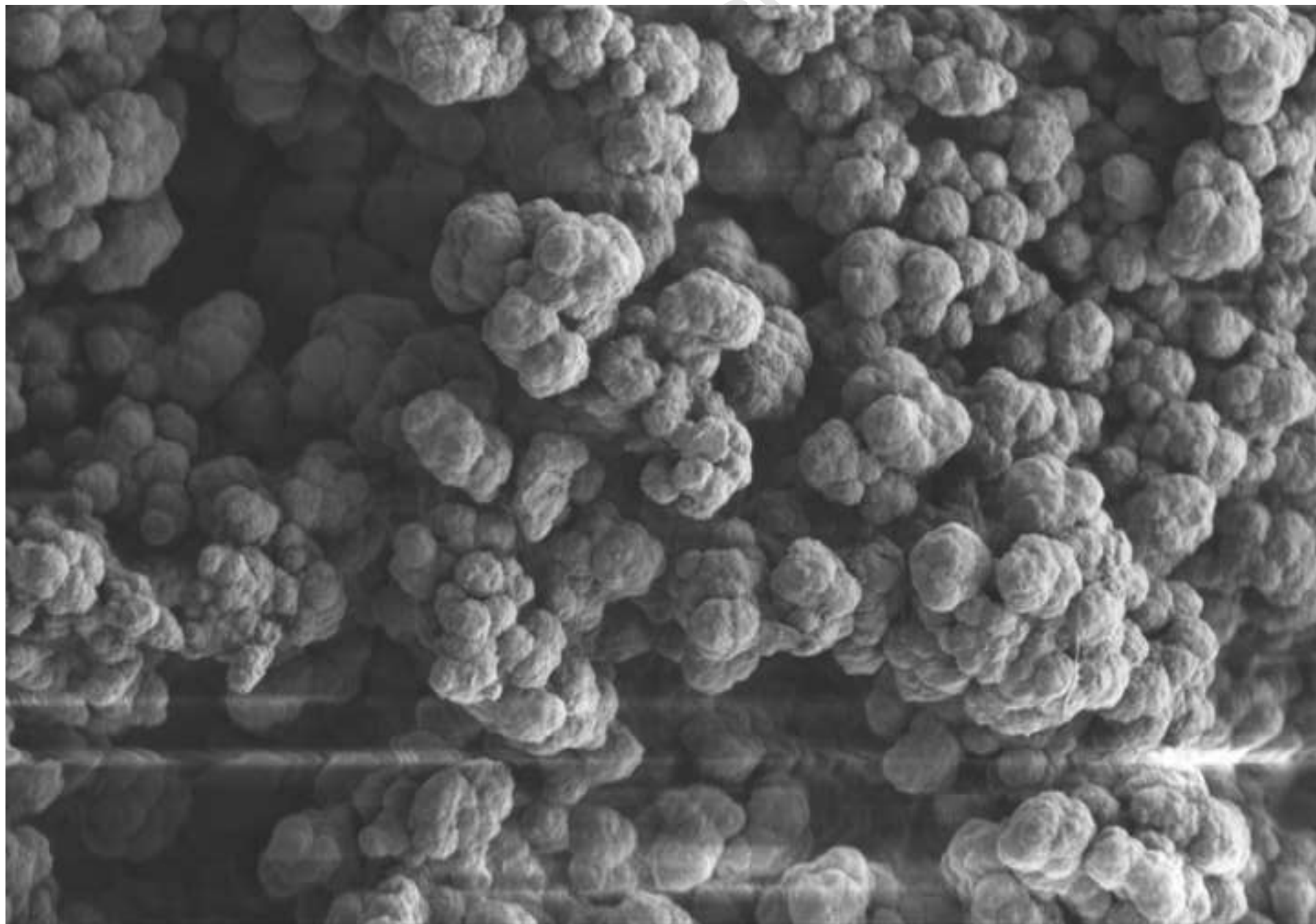
Accepted Manuscript

Figure 1a



GIEC80-99 1.0kV 9.4mm x900 SE(L) 2014-3-28 16:49 50.0um

Figure 1b



GIEC80-00 1.0kV 9.4mm x3.50k SE(L) 2014-3-28 16:51 10.0um

Fig. 2

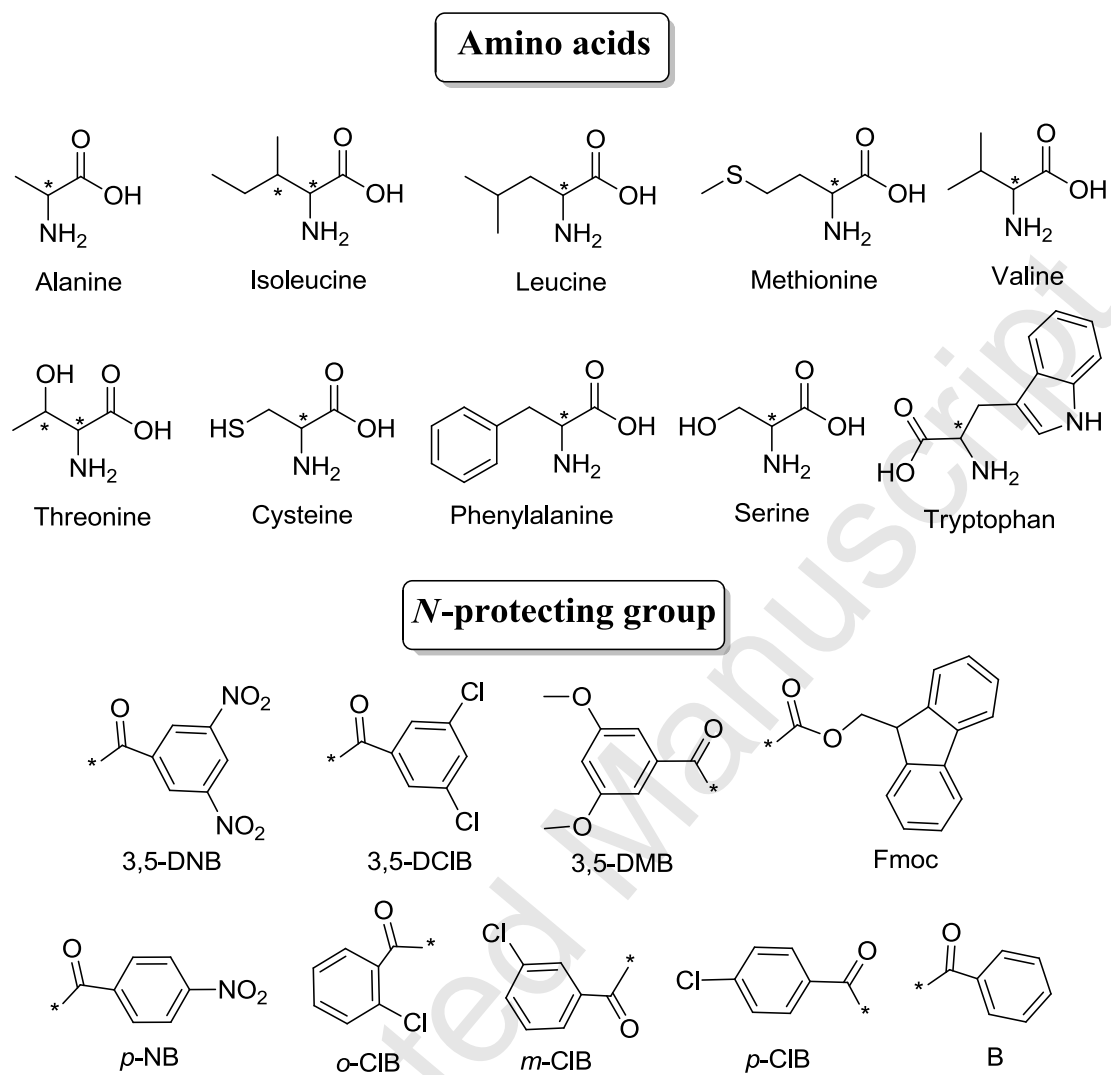
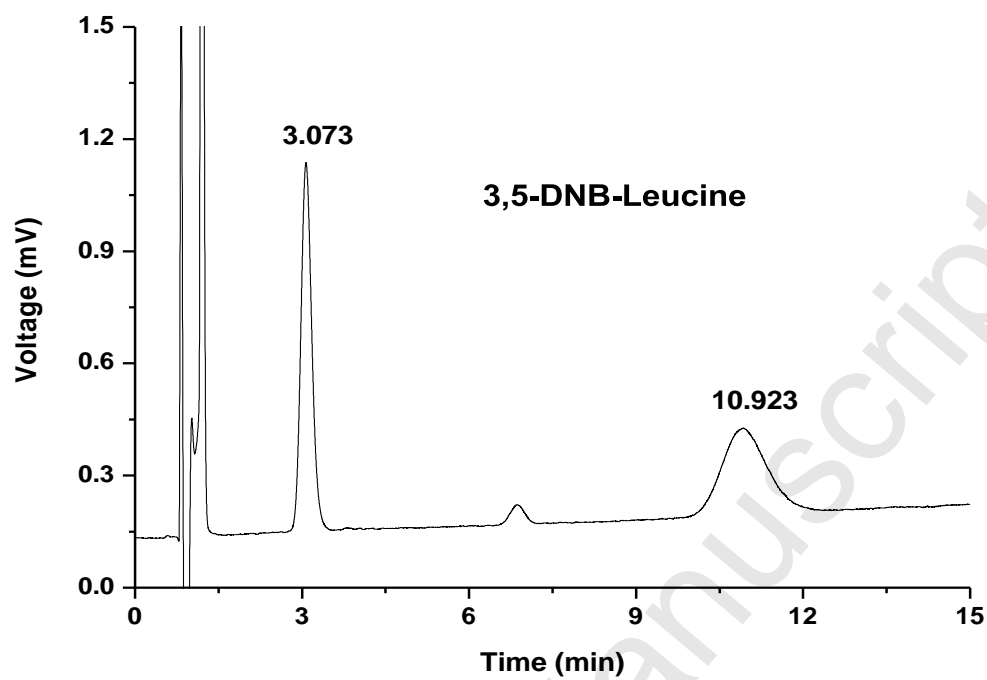
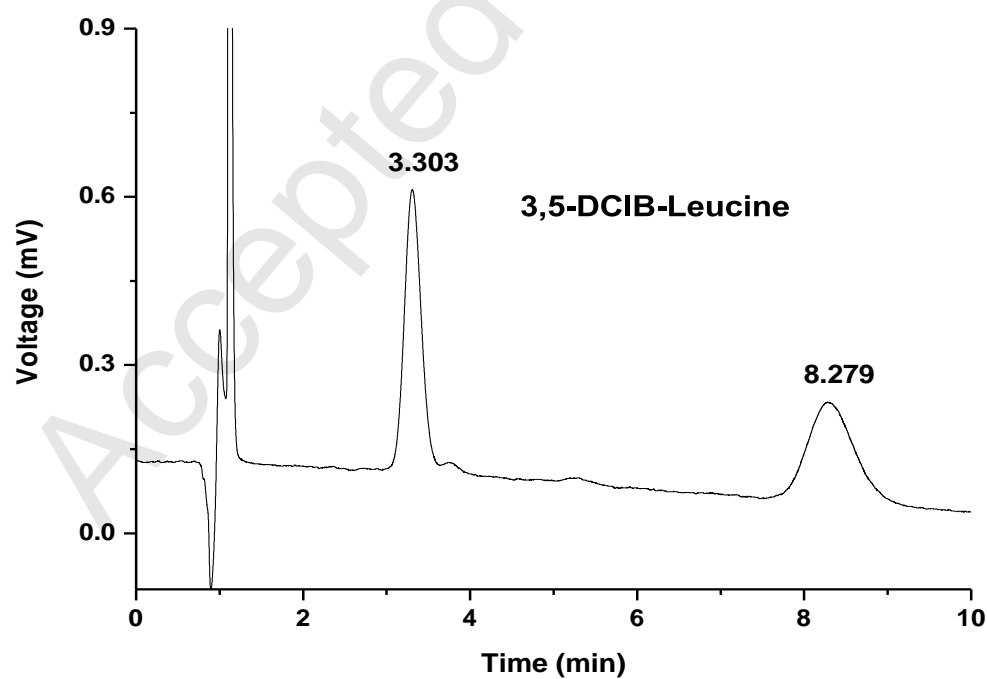


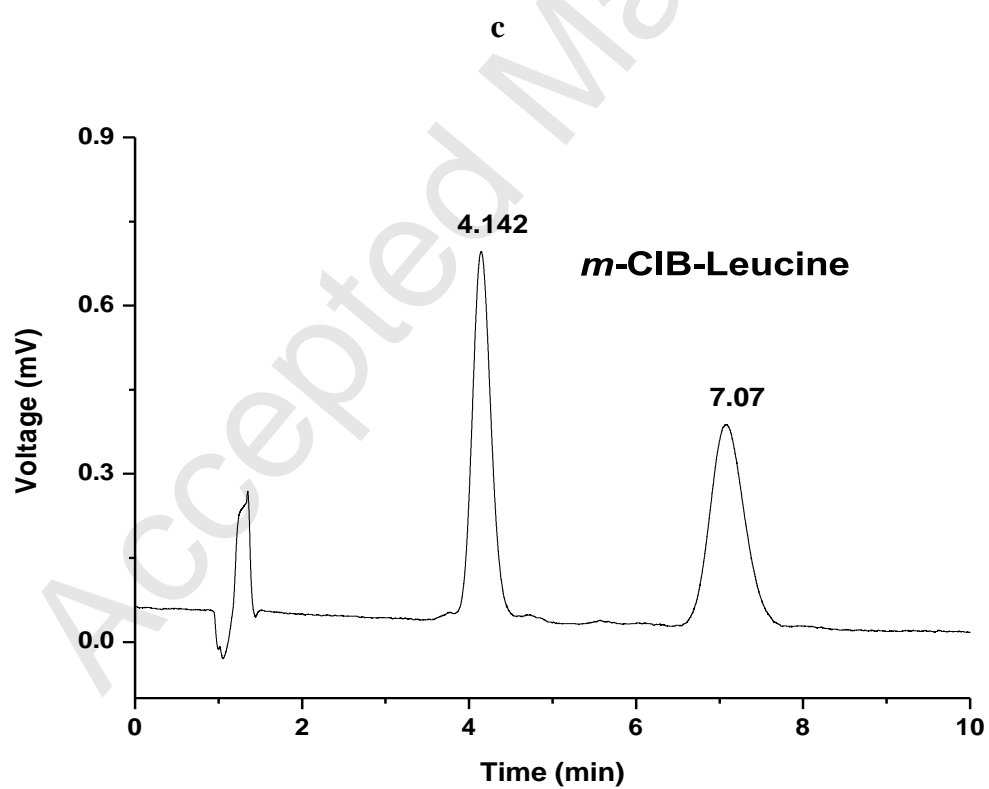
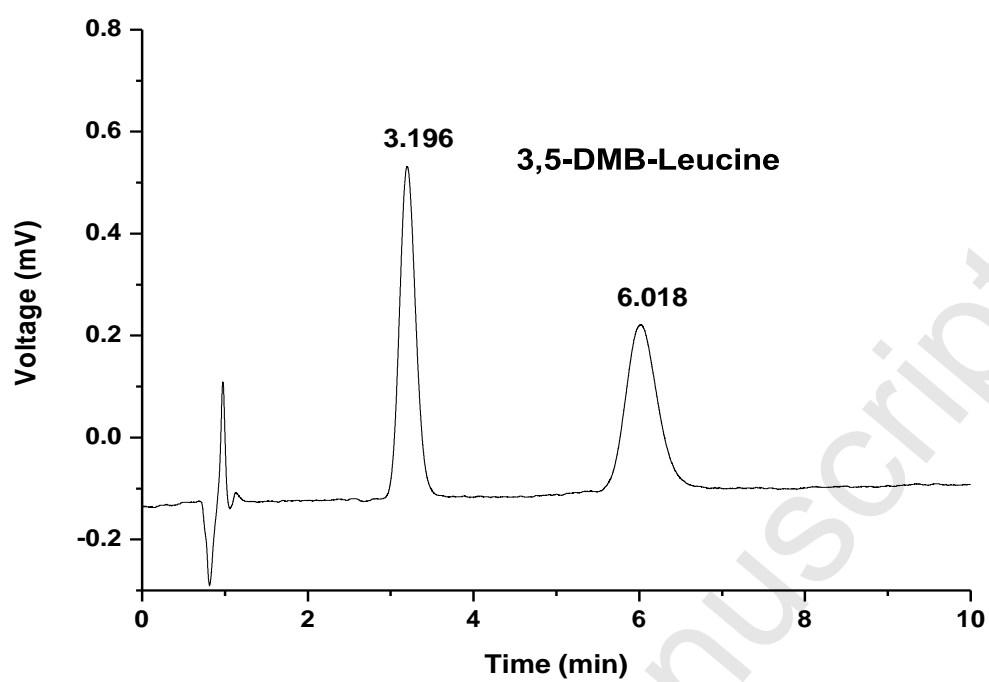
Fig. 3



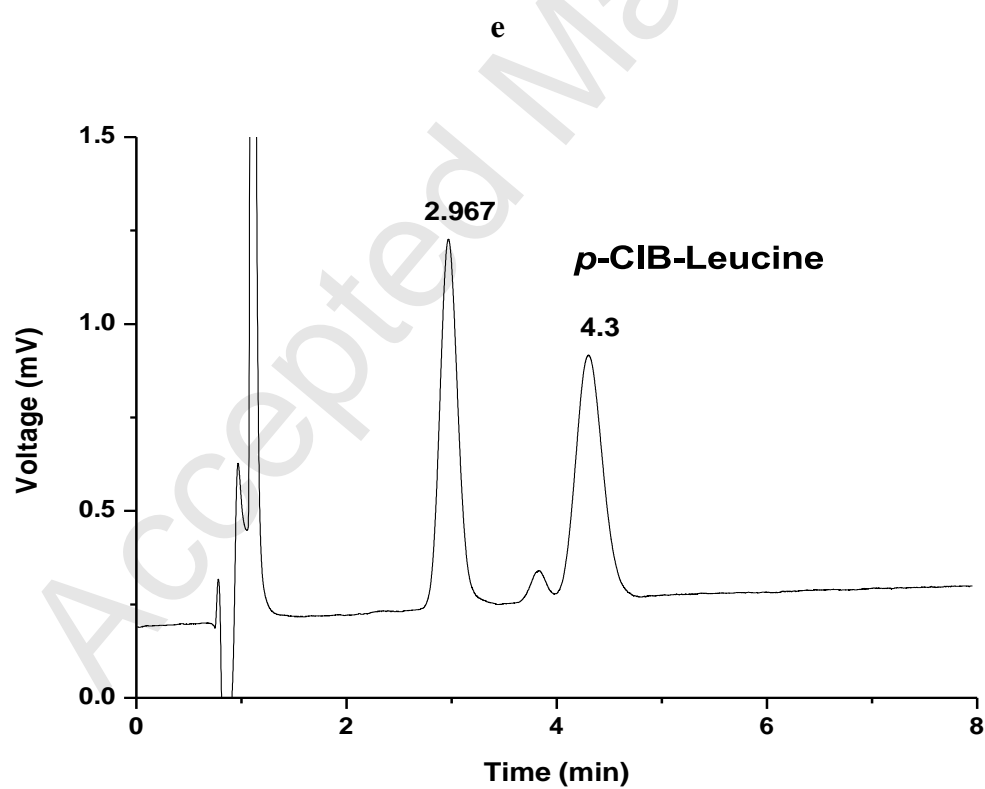
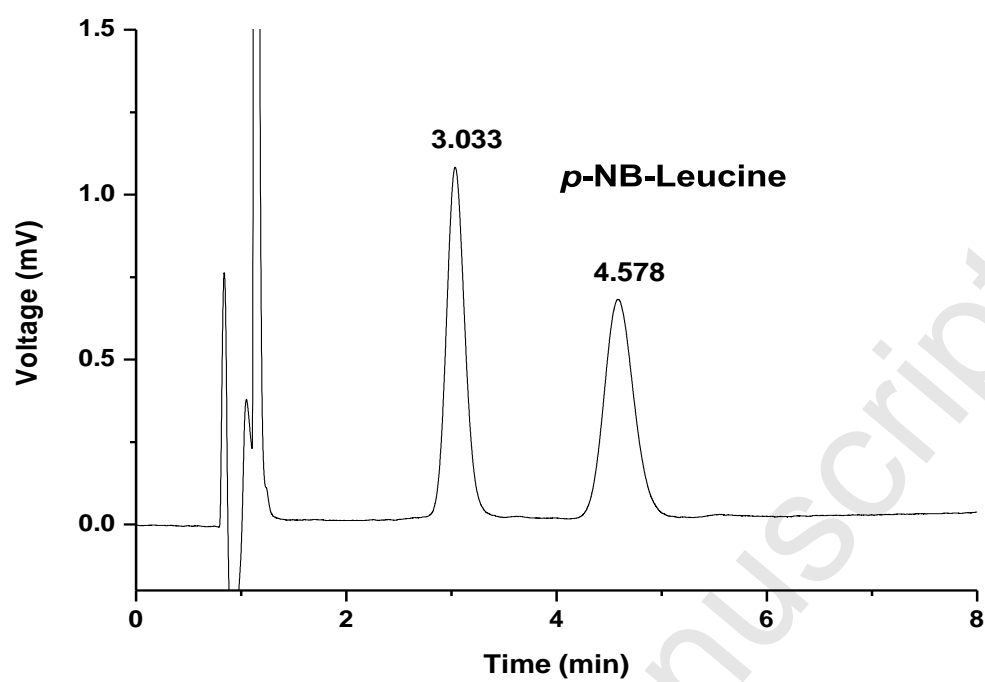
a



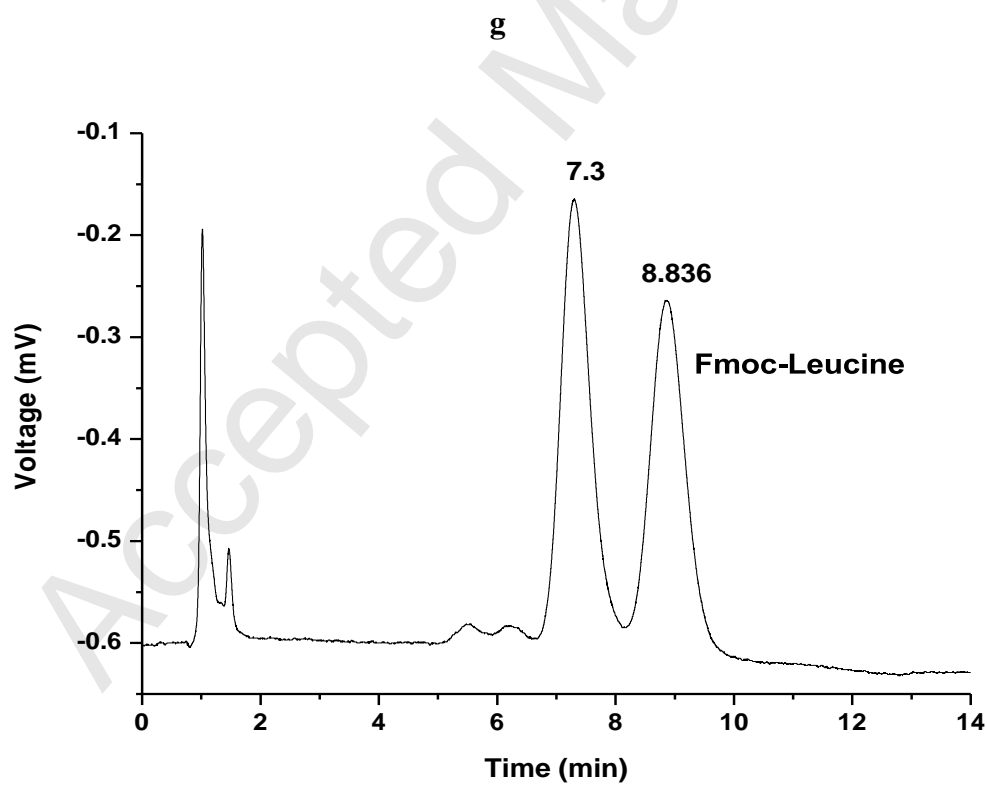
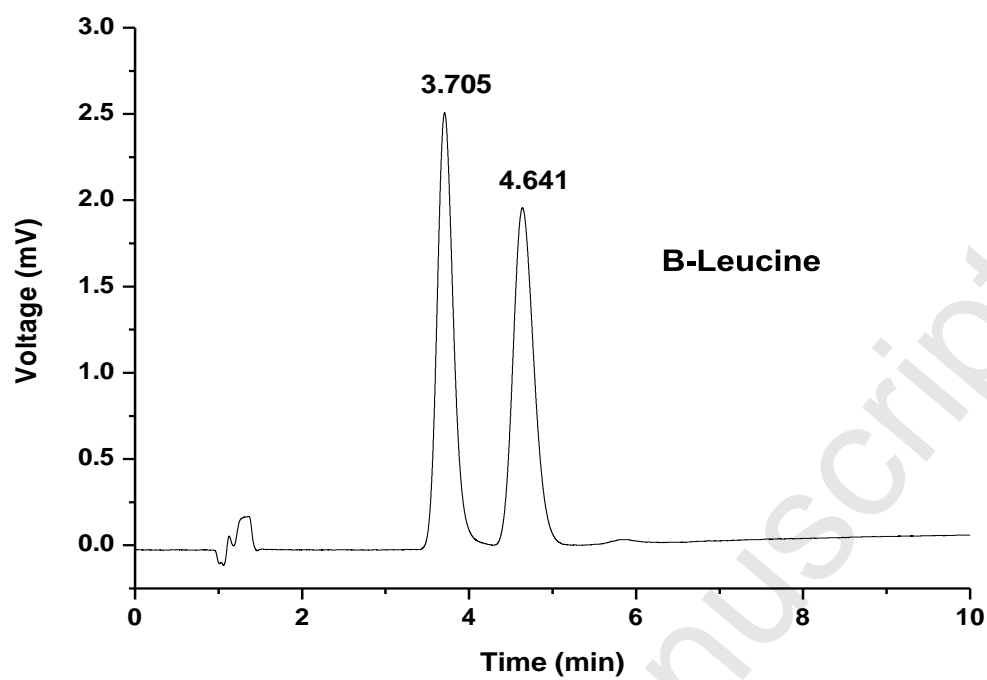
b



d

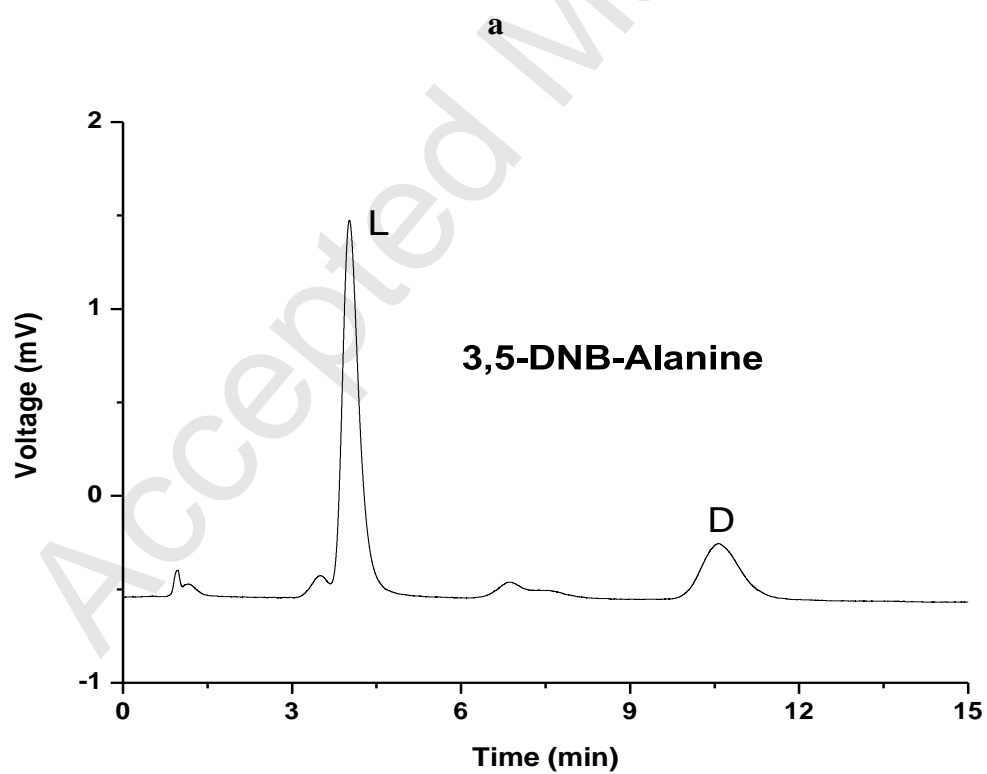
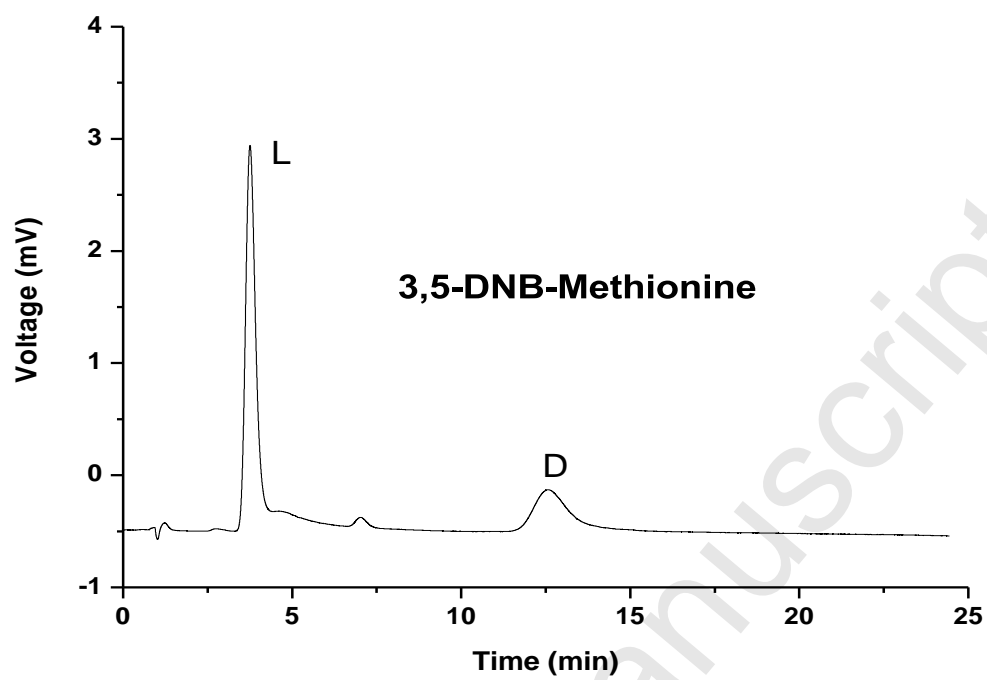


f



h

Fig. 4



b

Fig. 5

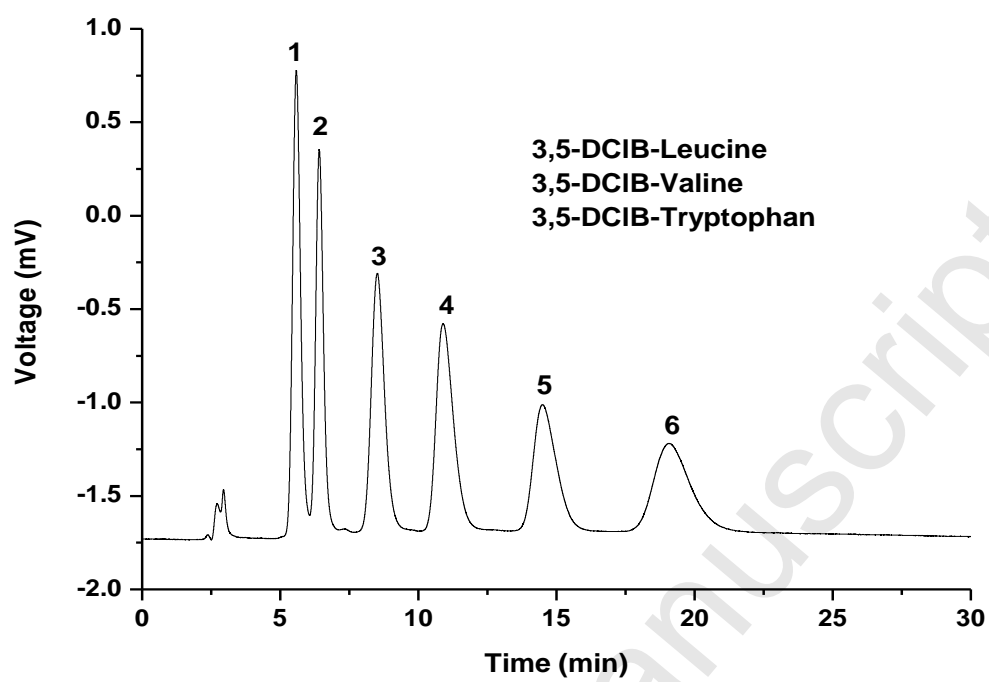


Table 1. Composition of the polymerization mixtures used for the preparation of poly(MQD-*co*-HEMA-*co*-EDMA) monolithic columns and their properties.

Column	Monomers (% w/w)			Porogens (% w/w)		Monomers : Porogens (% w/w)		Back-pressure (MPa)	Theoretical plates (m ⁻¹)
	MQD	HEMA	EDMA	Dodecanol	Cyclohexanol				
C1	20	52.5	27.5	83.33	16.67	30	70	2.9	20600
C2	20	52.5	27.5	83.33	16.67	35	65	5.4	24400
C3	20	52.5	27.5	83.33	16.67	40	60	10.1	21000
C4	20	55	25	83.33	16.67	35	65	5.6	26500
C5	20	57.5	22.5	83.33	16.67	35	65	6.2	32000
C6	20	60.0	20.0	83.33	16.67	35	65	19.2	26200
C7	20	57.5	22.5	88.33	11.67	35	65	5.8	20500
C8	20	57.5	22.5	78.33	21.67	35	65	13.1	20700

Conditions: column dimensions: 150 mm × 100 μm I.D.; mobile phase, ACN/H₂O (40/60, v/v); UV detection wavelength: 214 nm; flow rate: 1 μL/min; injection volume: 20 nL; sample: naphthalene.

Table 2. Permeability of the poly(MQD-*co*-HEMA-*co*-EDMA) monolithic column

Mobile phase	Relative polarity^[a]	Viscosity η ($\times 10^{-3}$ Pa·s)[32]	Permeability K ($\times 10^{-13}$ m²)
ACN	0.460	0.369	1.547
MeOH	0.762	0.544	1.024
Water	1	0.890	0.839

^a Relative polarity data were obtained from <http://virtual.yosemite.cc.ca.us/smurov/orgsoltab.htm>; viscosity data of pure solvents were obtained from reference [32].

Table 3. Effect of ACN content in the mobile phase on the retention and enantioseparation of *N*-derivatized amino acids.

	80%						70%						60%					
	k_1	k_2	α	R_s	N_1/m	N_2/m	k_1	k_2	α	R_s	N_1/m	N_2/m	k_1	k_2	α	R_s	N_1/m	N_2/m
3,5-DNB-Leucine	1.00	4.71	4.71	8.51	16600	8600	1.71	7.70	4.52	9.60	15400	9662	2.56	11.97	4.67	11.40	19400	11700
3,5-DCIB-Leucine	1.01	3.15	3.12	6.64	16100	10200	1.88	5.67	3.03	8.04	15100	12377	2.94	9.16	3.11	9.69	20200	14100

Conditions: column: 150 mm \times 100 μ m I.D. poly(MQD-*co*-HEMA-*co*-EDMA); mobile phase: mixture of ACN and 0.1 M ammonium acetate at various ratios (apparent pH = 5.3); UV detection wavelength: 254 nm; flow rate: 1 μ L/min; injection volume: 20 nL.

Table 7. Comparison of retention factor, selectivity and enantioresolution of different *N*-derivatized leucine derivatives.

Analyte	k_1	k_2	α	R_s
3,5-DNB-Leucine	1.00	4.71	4.71	8.51
3,5-DCIB-Leucine	1.01	3.15	3.12	6.64
3,5-DMB-Leucine	2.35	5.31	2.26	5.30
<i>m</i> -CIB-Leucine	3.35	6.42	1.92	4.94
<i>p</i> -NB-Leucine	2.18	3.80	1.74	3.68
<i>p</i> -CIB-Leucine	2.11	3.51	1.66	3.34
B-Leucine	2.89	3.87	1.34	2.31
Fmoc-Leucine	6.66	8.27	1.24	1.53

Conditions as in **Fig. 3**.

Table 4. Effect of the mobile phase apparent pH on the retention and enantioseparation of *N*-derivatized amino acids.

	pH 6.3						pH 5.3						pH 4.3					
	k_1	k_2	α	R_s	N_1/m	N_2/m	k_1	k_2	α	R_s	N_1/m	N_2/m	k_1	k_2	α	R_s	N_1/m	N_2/m
3,5-DNB-Leucine	2.26	10.55	4.68	10.52	14600	10600	1.00	4.71	4.71	8.51	16600	8600	0.48	1.91	3.96	4.36	7200	5200
3,5-DCIB-Leucine	4.60	14.22	3.09	8.80	12200	11500	1.01	3.15	3.12	6.64	16100	10200	0.49	1.25	2.55	3.01	8100	6400

Conditions: mobile phase, ACN/0.1 M ammonium acetate (80/20, v/v) adjusted to different apparent pH values; other conditions as in **Table 3**.

Table 5. Effect of the buffer concentration on the retention and enantioseparation of *N*-derivatized amino acids.

	0.15 M						0.10 M						0.05 M					
	k_1	k_2	α	R_s	N_1/m	N_2/m	k_1	k_2	α	R_s	N_1/m	N_2/m	k_1	k_2	α	R_s	N_1/m	N_2/m
3,5-DNB-Leucine	0.77	3.63	4.70	7.75	13600	8600	1.00	4.71	4.71	8.51	16600	8600	1.71	7.88	4.61	10.38	15000	11500
3,5-DCIB-Leucine	0.73	2.36	3.22	6.05	14000	10500	1.01	3.15	3.12	6.64	16100	10200	1.70	5.40	3.18	7.94	17900	10600

Conditions: ACN/different concentrations of ammonium acetate (80/20, v/v) (apparent pH = 5.3); other conditions as in **Table 3**.

Table 6. Enantioseparation of *N*-derivatized amino acids.

Sapmle	k_1	k_2	α	R_s	N_1/m	N_2/m
3,5-DNB-Isoleucine ^a	2.56	17.88	6.98	8.74	4500	4200
3,5-DNB-Valine ^a	2.93	16.26	5.55	8.92	7400	5000
3,5-DNB-Tryptophan ^a	4.43	22.00	4.97	7.32	4400	3600
3,5-DNB-Leucine ^a	1.00	4.71	4.71	8.51	16600	8600
3,5-DNB-Phenylalanine ^a	3.27	15.21	4.65	9.95	4900	4200
3,5-DNB-Methionine ^a	3.05	13.24	4.33	8.09	8400	5100
3,5-DNB-Threonine ^a	3.86	14.07	3.64	8.14	6000	6700
3,5-DNB-Cysteine ^a	5.68	19.88	3.50	4.31	2000	1900
3,5-DNB-Alanine ^a	3.55	11.30	3.19	8.06	10700	7400
3,5-DNB-Serine ^a	4.52	14.05	3.11	8.47	10500	8400
3,5-DCIB-Isoleucine ^a	1.31	5.58	4.24	8.71	17100	9200
3,5-DCIB-Valine ^a	1.39	4.76	3.42	8.74	19200	12800
3,5-DCIB-Phenylalanine ^a	2.29	7.65	3.33	8.17	15400	9400
3,5-DCIB-Leucine ^a	1.01	3.15	3.12	6.64	16100	10200
3,5-DCIB-Tryptophan ^a	2.33	7.13	3.06	6.87	10400	8000
3,5-DCIB-Methionine ^a	1.39	4.10	2.95	7.33	13300	13100
3,5-DCIB-Threonine ^a	2.15	5.52	2.57	8.00	21000	15400
3,5-DCIB-Cystenine ^a	3.41	7.78	2.28	5.22	14000	6300
3,5-DCIB-Alanine ^a	1.94	4.30	2.21	6.79	22100	16300
3,5-DCIB-Serine ^a	2.70	5.88	2.18	7.55	23800	18800
Fmoc-Isoleucine ^b	9.58	13.50	1.41	2.90	9700	8800
Fmoc-Valine ^b	8.20	11.47	1.40	2.76	9100	8600

Fmoc-Phenylalanine ^b	9.33	11.82	1.27	1.84	7800	7600
Fmoc-Cysteine ^c	13.91	17.61	1.27	1.58	5500	5400
Fmoc-Tryptophan ^b	12.18	15.33	1.26	1.69	7100	6300
Fmoc-Leucine ^b	6.66	8.27	1.24	1.53	6900	6900
Fmoc-Serine ^b	4.43	5.47	1.23	1.56	9100	8300
Fmoc-Methionine ^b	5.82	7.08	1.22	1.43	7700	7500
Fmoc-Alanine ^c	8.40	9.77	1.16	1.38	10100	9900
3,5-DMB-Leucine ^a	2.35	5.31	2.26	5.30	8300	7800
3,5-DMB-Methionine ^a	2.12	4.20	1.98	4.50	9500	8100
3,5-DMB-Alanine ^a	2.06	3.53	1.71	3.98	12700	10300
<i>p</i> -NB-Leucine ^a	2.18	3.80	1.74	3.68	9400	8300
<i>p</i> -NB-Methionine ^a	2.74	4.43	1.62	3.75	11500	10500
<i>p</i> -NB-Threonine ^a	3.93	5.87	1.49	3.91	15500	14700
<i>p</i> -NB-Alanine ^a	2.69	3.84	1.43	3.08	14100	13800
<i>m</i> -ClB-Leucine ^a	3.35	6.42	1.92	4.94	11000	8800
<i>m</i> -ClB-Threonine ^a	3.44	5.72	1.67	4.43	12600	12600
<i>m</i> -ClB-Alanine ^a	3.08	4.67	1.52	3.72	14200	13400
<i>m</i> -ClB-Methionine ^a	2.83	3.70	1.31	2.22	12800	12400
<i>p</i> -ClB-Leucine ^a	2.11	3.51	1.66	3.34	9400	8400
<i>p</i> -ClB-Methionine ^a	3.03	4.62	1.52	3.53	12600	11900
<i>p</i> -ClB-Alanine ^a	2.95	4.02	1.36	2.87	16100	14700
B-Leucine ^a	2.89	3.87	1.34	2.31	11800	10900
B-Methionine ^a	2.81	3.67	1.31	2.17	12500	11700
B-Threonine ^a	4.25	5.32	1.25	2.27	16400	15500

<i>o</i> -ClB-Methionine ^a	5.83	6.30	1.08	0.74	/	/
---------------------------------------	------	------	------	------	---	---

Conditions: mobile phase, ^aACN/0.1 M ammonium acetate solution (80/20, v/v) (apparent pH = 5.3); ^b ACN/0.1 M ammonium acetate (50/50, v/v) (apparent pH = 5.3); ^c ACN/ 0.1 M ammonium acetate (40/60, v/v) (apparent pH = 5.3); other conditions as in **Fig. 3**; “/”: the number of theoretical plates cannot be calculated.

Accepted Manuscript